Nucleon-antinucleon annihilation via confined quark-gluon states

R. Tegen
Department of Physics and Astronomy, University of South Carolina, Columbia, South Carolina 29208

T. Mizutani
Department of Physics, Virginia Polytechnic Institute and State University, Blacksburg, Virginia 24061

F. Myhrer
Department of Physics and Astronomy, University of South Carolina, Columbia, South Carolina 29208
(Received 15 October 1984; revised manuscript received 25 February 1985)

In this work we use the quark degrees of freedom in a nucleon to calculate a nucleon-antinucleon annihilation potential. The range of this annihilation is determined by the long-range confinement forces giving the quark wave functions which also reproduce the nucleon charge radius. We find that $N\bar{N}$ scattering is sensitive to the annihilation mainly between 0.5 and 2.0 fm. Our annihilation model shows that the dominant annihilation contribution to $N\bar{N}$ scattering comes from $qq\bar{q}\,\bar{q}$ multigluon intermediate states and that the intermediate $q\bar{q}$ multigluon as well as pure gluonic states are less important for $N\bar{N}$ scattering.

I. INTRODUCTION

The nucleon-antinucleon ($N\bar{N}$) interaction at low energy is dominated by the annihilation process but the ratio of the total elastic to total cross section indicates that we have some real, attractive forces extending beyond a possible black sphere characterizing the annihilation. At higher energies meson production becomes important and $p\bar{p}$ and pp scattering both become similar, dominated by diffractive particle production. From the chiral quark models[1,2] we know that the nucleon has a quark core surrounded by a pion cloud. These models have been very successful in describing static hadronic properties[3,4] and nucleon charge and axial-vector form factors,[5] and give us a hint as to how to understand nucleon-antinucleon low-energy scattering; for scattering with a large impact parameter (large l partial waves) we should expect mainly the meson clouds to interact and the standard one-boson-exchange potential (OBEP) should be a reasonable approximation. However, for small impact parameters the two quark cores in N and $\bar{N}$ should overlap. This means that we may not completely understand the low $N\bar{N}$ partial wave scattering without including the quark degrees of freedom. Here we immediately have a nice picture complementing the early dispersion argument of Martin[6] as to why the annihilation forces are a short-distance phenomenon: the $N\bar{N}$ only annihilate when the two quark cores overlap. These arguments are in line with the proposed coupled-channel nucleon-nucleon (NN) description of, e.g., Simonov[7] or Lomon,[7] who try to resolve the ambiguous dual picture of treating nucleon-nucleon scattering through meson exchanges as well as via quark-quark interactions. As a first step the simple $N\bar{N}$ black-sphere annihilation model (complemented with a meson-exchange potential for longer distances) of Dalkarov and Myhrer[8] fits nicely into this modern understanding. In a previous work[9] we have compared a few $N\bar{N}$ model descriptions with data. One interesting result in that work, relevant to the present argument, is that at backward $p\bar{p}$ scattering simple annihilation models deviate from data. This might indicate the need for a dynamical description of the annihilation process, which we will start developing in this work.

In the following we will show that the long-range QCD confinement forces determine the range of the annihilation process. In this work we use the MIT bag model[18] or the Regensburg scalar confinement potential[19] to derive the radial dependence of an annihilation potential. The quark-antiquark annihilation into one or more hard, but confined, gluons is presumably of very short range and can therefore be calculated perturbatively. The annihilation of two or more $q\bar{q}$ pairs into two or more gluons is also calculated (in the coherent approximation) and we will discuss the radial dependence of these processes for $p\bar{p}$ scattering. As we will discuss, the radial dependences of the different processes are mainly determined by quark confinement which already includes implicitly the bulk of the soft multigluon effects. We will argue that these processes only enter in determining the effective annihilation strength required to describe $N\bar{N}$ scattering data.

Several groups have considered the quark-rearrangement model.[10,11] We prefer as a start to explicitly use a model with more dynamics involved in order to understand this annihilation process better following early suggestions in this direction.[12,13] Both from topological arguments[14(a)] and in the $1/N$ expansion[14(b)] nonplanar diagrams (like the rearrangement diagrams) are considered higher-order corrections to planar diagrams. For discussions on these points see Rossi[14(c)] and a recent discussion based on the $^3P_0$ annihilation model by Dover and Fishbane.[14(d)] As stated, we will here as a first approximation consider the planar one-gluon and two-gluon an-

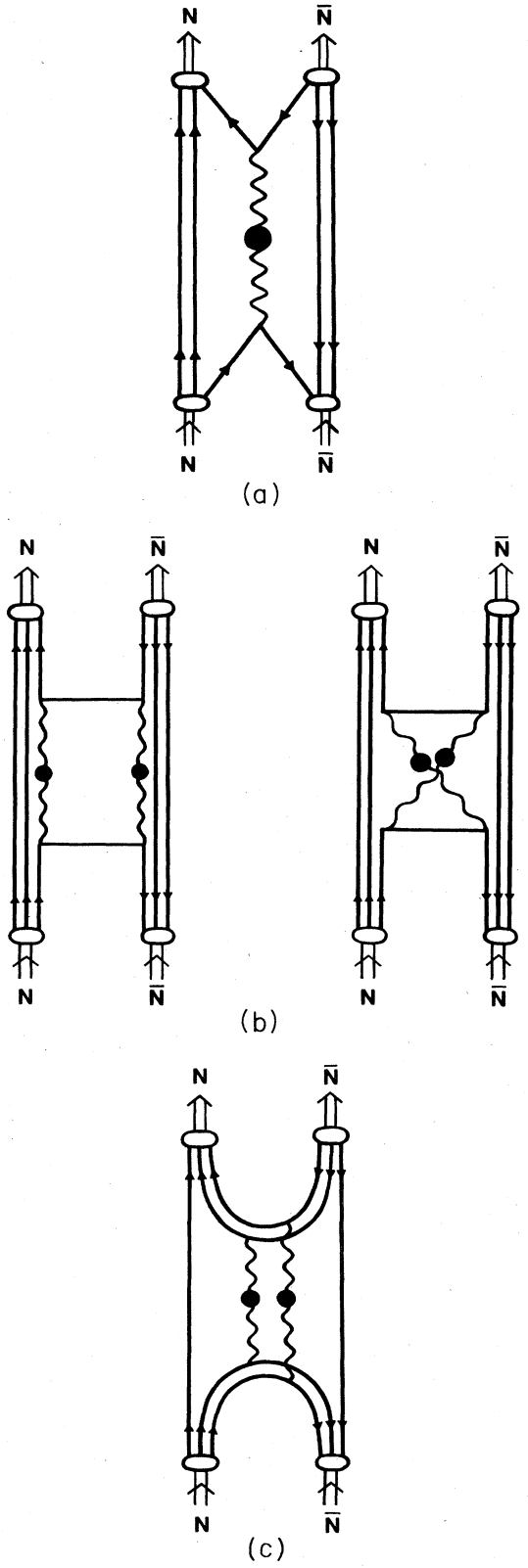

FIG. 1. The planar $N\bar{N}\rightarrow$mesons$\rightarrow N\bar{N}$ annihilation diagrams discussed here in (a) the $q\bar{q}\rightarrow$confined one gluon approximation, (b) $q\bar{q}\rightarrow$two gluon, box and crossed box, and (c) $q\bar{q}q\bar{q}\rightarrow$two gluon.

nihilation channels of Figs. 1(a)—1(c). The chiral potential quark models and the chiral bag models require the presence of the pion, and one finds that in all these models the source of the pion is surface peaked and the pion field is suppressed inside the quark confinement region. This pion field which is demanded by the underlying chiral symmetry, however, does not contribute directly to the $N\bar{N}$ annihilation but is included in the *long-range* part of the $N\bar{N}$ OBEP. This means that in addition to the annihilation optical potential, where the annihilation is supposed to proceed via intermediate confined antiquark-quark-gluon states, we assume that the real $N\bar{N}$ potential is the G-parity-transformed meson-exchange potential of either Bryan and Phillips,[15] Nijmegen's D model,[16] or the static Paris potential of Richard;[17] all three meson-exchange models are discussed in our previous work.[9]

In the following section we will first present our calculation of the quark-gluon annihilation model. Then in Sec. III we will use this optical annihilation model together with the long-range meson-exchange potential to describe the data. We draw our conclusions in Sec. IV.

II. THE CONFINED GLUON ANNIHILATION MODEL

From our introduction it should be clear that for small impact parameters the $N\bar{N}$ interaction has to be explained by the quark (antiquark) and gluon content of the nucleon (antinucleon). Quarks and gluons are confined within a nucleon and this may be described either by various bag models[2–4,18] or by the scalar confinement potential model[19] where effectively the quarks are given an r-dependent mass $M(r)=cr^n$ ($n=2,3$), where r is the distance of a quark (antiquark) from the center of mass of the nucleon (antinucleon). Common to all these models is that $N\bar{N}$ annihilation proceeds only when the N and $\bar{N}$ confinement regions (or bags) overlap so that q and $\bar{q}$ can annihilate into gluons which hadronize into mesons. Scalar confinement potential models[19] do not have a sharp surface like the bag model, but the quark density dies out very rapidly beyond a certain distance r_0 which we define as the quark-core size. The overlap between N and $\bar{N}$ in the potential model will largely be determined by the magnitude of the quark (antiquark) annihilation density for a given separation of N and $\bar{N}$ (see below).

In the following we will first calculate the imaginary (i.e., annihilation) part of the $N\bar{N}$ potential in the $\bar{q}q\rightarrow$one-confined-gluon approximation [see Fig. 1(a)] (an interaction of a very short range which should be described in perturbative QCD). Our approach is different from previous ones[12,13] in that we investigate several chiral quark models, the chiral bag model,[2–4] and the scalar confinement potentials[19] $M(r)=cr^n$. In addition we take into account the confinement effect on the gluon propagator. Secondly, we calculate the $q\bar{q}\rightarrow$two-gluon process in the coherent approximation. The radial dependence of the annihilation potential thus obtained allows for a *direct* physical interpretation in terms of a quark (antiquark) annihilation-density function which is described by the long-range QCD forces, and short-range

QCD coupling α_s and the confined gluon's "effective mass." The annihilation depends not only on the size of the QCD coupling α_s but also on the confined quark annihilation density function which already includes the bulk of soft multigluon effects and our studies indicate that annihilation of one $q\bar{q}$ pair into two or more hard but confined gluons within our approximations have basically the same radial annihilation dependences in $N\bar{N}$ scattering. Detailed studies of these multigluon annihilation channels is under way.

$$\mathscr{L}_{\rm int}(x)=\sqrt{4\pi\alpha_s}\,\overline{\psi(x)}\gamma^\mu\frac{\lambda_a}{2}\psi(x)G^a_\mu(x) \tag{1}$$

we calculate first the contribution of diagrams Figs. 2(a) and 2(b) to the $N\bar{N}$ annihilation potential $V(r)$. We have to evaluate the matrix

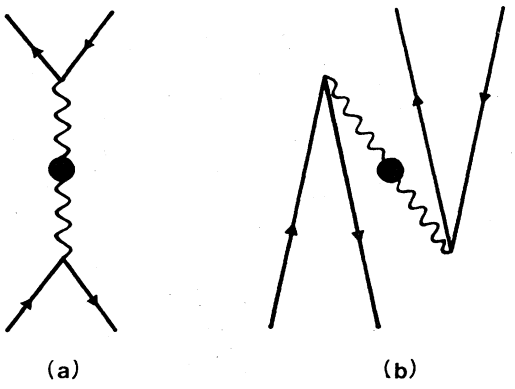

FIG. 2. Feynman diagrams for the subprocess $q\bar{q}\to G^*\to q\bar{q}$.

$$M=\int\int d^4r_1 d^4r_1'\left\langle N\bar{N}\left|\sqrt{4\pi\alpha_s}\,\bar{u}\left[r_1'-\frac{r}{2}\right]\gamma^\nu\frac{\lambda_b}{2}v\left[r_1'+\frac{r}{2}\right]iD^{ba}_{\nu\mu}(r_1'-r_1)\sqrt{4\pi\alpha_s}\,\bar{v}\left[r_1+\frac{r}{2}\right]\gamma^\mu\frac{\lambda_a}{2}u\left[r_1-\frac{r}{2}\right]\right|N\bar{N}\right\rangle, \tag{2}$$

where $\mathbf{r}$ is the relative distance between the N and $\bar{N}$ centers and where $D^{ab}_{\mu\nu}(z)$ is the confined gluon propagator, in terms of the spin-one part of the spectral functions $\rho^{(1)}$, viz.,

$$iD^{ab}_{\mu\nu}(z)=\delta^{ab}\int\frac{d^4q}{(2\pi)^4}e^{-iq\cdot z}\int d\sigma\rho^{(1)}(\sigma)\frac{g_{\mu\nu}-q_\mu q_\nu/\sigma}{q^2-\sigma+i\epsilon} \tag{3}$$

and the wave functions u and v are solutions of the bound Dirac equation,

$$[i\partial_x-M(x)]u(x)=0=[i\partial_y+M(y)]v(y) \tag{4}$$

with the confinement coordinates (the time-dependent part of u,v is $e^{\mp iEt}$, as usual) $\mathbf{x}=\mathbf{r}_1-\mathbf{r}/2$, $\mathbf{y}=\mathbf{r}_1+\mathbf{r}/2$ (see Fig. 3) and the confining potential $M(x)=c\,|\,\mathbf{x}\,|^n(n=2,3)$. The evaluation of M, Eq. (2), becomes more transparent if we define a form factor as

$$F^\mu_a(\mathbf{q},\mathbf{r})\equiv\int d^3y\,e^{-i\mathbf{q}\cdot\mathbf{y}}\left\langle\bar{v}(\mathbf{y})\gamma^\mu\frac{\lambda_a}{2}u(\mathbf{y}-\mathbf{r})\right\rangle \tag{5}$$

which describes the vertex for $q\bar{q}$ annihilation into a gluon where the $\mathbf{r}$ dependence is due to the important fact that the gluon couples to a quark and an antiquark which are confined with respect to *different* centers (c.m. of N and $\bar{N}$, respectively, which are separated by a distance $\mathbf{r}$). Another observation is the magnitude of the four-momentum transfer $q_\mu=(q_0,\mathbf{q})$ of the quark-antiquark to the gluon. In the center-of-mass system of N and $\bar{N}$ the annihilating $q\bar{q}$ pairs will have equal and opposite momenta (apart from internal Fermi motion). Hence, the momentum transfer $\mathbf{q}$ to the gluon can only come from their Fermi momenta inside their confinement domains in the nucleon and antinucleon, respectively. Since the energy $E_0,\bar{E}_0$ of lowest-lying $1S_{1/2}$ quarks and antiquarks in their confining potential $M(r)=cr^n$ is 500–600 MeV, their energy transfer q_0 is larger than ~ 1 GeV and hence on the average larger than their Fermi momenta (~ 270 MeV/c). Within the confined one-gluon annihilation approximation we therefore neglect the momentum transfer $\mathbf{q}$ to the gluon as compared to the energy transfer q_0.

With this approximation in mind F^μ_a is easily evaluated, $\mu=\{{0\atop k}\}$,

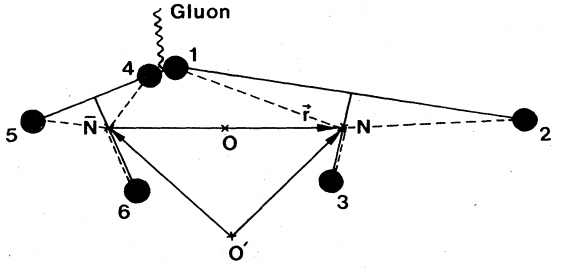

FIG. 3. $N\bar{N}$ kinematics. N (quarks 1,2,3), $\bar{N}$ (antiquarks 4,5,6), $\mathbf{r}=\mathbf{R}_N-\mathbf{R}_{\bar{N}}$; in the c.m. system of $N\bar{N}$ $\mathbf{R}\equiv\frac{1}{2}(\mathbf{R}_N+\mathbf{R}_{\bar{N}})=0$, $\mathbf{R}_N=\mathbf{r}/2=-\mathbf{R}_{\bar{N}}$.

$$F_a^{\mu}(\,|\,\mathbf{q}\,|\ll q_0,\mathbf{r})=\rho(\mathbf{r})\left\langle \sum_{\substack{i=1,2,3\\ j=4,5,6}} (-1)^{-m_j}\chi^{\dagger}(-m_j)\begin{bmatrix}0\\ \sigma\end{bmatrix}\chi(m_i)\xi_j^{\dagger}\frac{\lambda_a}{2}\xi_i\right\rangle, \tag{6}$$

where $\rho(\mathbf{r})$ is our annihilation density function [see Eq. (7)], ξ is a SU(3) color spinor, and χ is a Pauli spinor-isospinor. In particular, $F_a^{\mu=0}(\mathbf{q}\equiv 0;\mathbf{r})\equiv 0$, which is exact. The result for the spatial part ($\mu=k$) is

$$F_a^{\mu=k}(\,|\,\mathbf{q}\,|\ll q_0;\mathbf{r})\sim\rho(\mathbf{r})\left\langle\chi^{\dagger}\sigma^k\chi\xi^{\dagger}\frac{\lambda_a}{2}\xi\right\rangle$$

up to terms which are proportional to the lower spinor component squared or higher. We neglect in this paper these correction terms since the one-gluon annihilation is already an approximation. The r dependence is then given by *one* function,

$$\rho(\mathbf{r})=\int\frac{d^3p}{(2\pi)^3}e^{i\mathbf{p}\cdot\mathbf{r}}\tilde{\rho}(\mathbf{p})\,, \tag{7a}$$

where

$$\tilde{\rho}(\mathbf{p})\equiv\phi^{\dagger}(\mathbf{p})\phi(\mathbf{p}) \tag{7b}$$

and $\phi(\mathbf{p})$ is the Fourier transform of the spatial part of the quark or antiquark spinor $u(\mathbf{r})$ or $v(\mathbf{r})$ (the time-dependent part is $e^{\pm iEt}$). In the matrix M, Eq. (2), the gluon propagator $D_{\nu\mu}^{ab}$ will be contracted with the following combinations of the form factor F^{μ}: $F_a^{\mu}(F_b^{\nu})^{\dagger}$.

To the extent that the momentum transfer $\mathbf{q}$ can be neglected relative to q_0, as discussed before Eq. (6), there is no ($\mu=0$, $\nu=0$) contribution to the matrix M, i.e., D_{00}^{ab} is irrelevant here. The gluon propagator in momentum space is then very simple since the contribution from the part $\sim q_{\mu}q_{\nu}/\sigma$ drops out for $\mathbf{q}^2\ll\sigma$. This is extremely important since this part of the gluon propagator is gauge dependent.[20] If the gluon spectral function $\rho^{(1)}(\sigma)$ is dominated by the lowest-lying gluon eigenstate (predictions range from $M_G^*=700$—1200 MeV for the lowest gluonic eigenmode in a cavity[21]), i.e., $\rho^{(1)}(\sigma)\sim\delta(\sigma-M_G^{*2})$, the approximation $\mathbf{q}^2\ll\sigma=M_G^{*2}$ is reasonable. The further evaluation of M is standard and we obtain with $\rho^{(1)}(\sigma)=g_G\delta(\sigma-M_G^{*2})$ the $N\bar{N}$ potential (effectively g_G depends on M_G^* in this approximation)

$$-V(r)=4\pi\alpha_s g_G\int\frac{d^3q}{(2\pi)^3}\frac{1}{2\omega_q}\sum_{\substack{a,b\\ i,j}}\delta^{ab}\delta_{ij}\left[\frac{F_a^i(\,|\,\mathbf{q}\,|\ll M_G^*;\mathbf{r})[F_b^j(\,|\,\mathbf{q}\,|\ll M_G^*;\mathbf{r})]^{\dagger}}{\omega_q-(E_0+\bar{E}_0)-i\epsilon}+\frac{F_a^i(\,|\,-\mathbf{q}\,|\ll M_G^*;\mathbf{r})[F_b^j(\,|\,-\mathbf{q}\,|\ll M_G^*;\mathbf{r})]^{\dagger}}{\omega_q+E_0+\bar{E}_0-i\epsilon}\right]_{\epsilon\to 0^+}, \tag{8}$$

where $\omega_q\equiv(\mathbf{q}^2+M_G^{*2})^{1/2}$ and g_G is the coupling strength of the gluon field in the one narrow state approximation.

Inserting (6) in Eq. (8) we obtain

$$V(r)=-4\pi\alpha_s g_G\rho^2(r)\left\langle N\bar{N}\left|\sum_{\substack{i=1,2,3\\ j=4,5,6}}\sigma(i)\cdot\sigma(j)\frac{\lambda(i)}{2}\cdot\frac{\lambda(j)}{2}\right|N\bar{N}\right\rangle\frac{1}{2\pi^2}\int_0^{\infty}dq\,q^2\frac{1}{\mathbf{q}^2+M_G^{*2}-(E_0+\bar{E}_0)^2-iM_G^*\Gamma_G}\,, \tag{9}$$

where we have introduced the gluon width Γ_G of the propagator. It is important to emphasize that this is an energy-dependent, effective doorway width for all the decaying processes: gluon + $qq\bar{q}\,\bar{q}\to$physical channels, which resembles the width of Δ in a nuclear medium as treated in the isobar doorway models of pion-nucleus interactions.[22] The color matrix element between color-singlet N and $\bar{N}$ states gives the familiar color factor $\frac{4}{3}$ and the function $\rho^2(r)$ is our r-dependent annihilation density.

We know that the annihilation will not only proceed through the one-gluon channel as in Ref. 13. We can easily have $q\bar{q}\to$two gluons as in Fig. 1(b), etc. In the approximation that the quark stays in its lowest confinement state (the coherent approximation) the radial form of, e.g., $q\bar{q}\to$two gluons$\to q\bar{q}$ [see Fig. 1(b)] will be $\rho^2(r)$, the same as in Eq. (9). [We have assumed that the quark wave functions vary slowly and can be taken outside the integral over one of the gluon propagator(s).[23]] The propagator integrals then only provide a constant coefficient in front of the $\rho^2(r)$ function. In the coherent approximation the graphs where one $q\bar{q}$ pair annihilates into three or more gluons[24] we also find a $\rho^2(r)$ behavior again assuming the r dependence from propagators to be slow compared to the quark wave-function variations. Since here one $q\bar{q}$ pair can go into one or two (Fig. 1) or several confined gluons and each of these graphs have different spin (angular momentum) isospin projection operators of different coefficients and we have to add the graphs, we will here as a first choice average over the different spin and isospin projection operators. *A priori* we do not know which graph, if any, will dominate the annihilation pro-

cess so we consider this to be a good first approximation. To make a definite statement about any dominance we also have to know how the intermediate multigluon $+qq\bar{q}\,\bar{q}$ states couple to mesons. This hadronization process should certainly give different energy-dependent weights to different graphs so we may not easily add the graphs of one $q\bar{q}$ into gluons like Figs. 1(a) and 1(b), etc. As just discussed, our intermediate gluons and quark-antiquark states are treated as doorway states decaying into physical channels. However, in the coherent approximation our result that all graphs have the same r dependence, $\rho^2(r)$, equal to that from the diagram in Fig. 1(a), allows us to make a very simple ansatz. We replace α_s by α_s^* (a free parameter) which means the $q\bar{q}$ into two or more gluons gives a constant in front of $\rho^2(r)$ and we also replace the one-gluon doorway width Γ_G by a new effective, energy-dependent doorway width Γ_G^*. Then our $N\bar{N}$ annihilation potential has the following form:

$$V(r)=-\tfrac{16}{3}\rho^2(r)\frac{\alpha_s^*}{\pi}g_G \times\int_0^\infty dq\,\mathbf{q}^2\frac{1}{\mathbf{q}^2+M_G^{*2}-(E_0+\bar{E}_0)^2-iM_G^*\Gamma_G^*}\,, \tag{10}$$

$$V(r)\equiv U(r)+iW(r)\,.$$

Since the different graphs in Fig. 1, etc., contribute very differently to the real part of $V(r)$ with different signs we have to calculate the explicit meson annihilation channels in this model using the same approximations that lead to Eqs. (10) and (11) in order to be able to be more specific about the energy dependence of the doorway width Γ_G^* and thereby about $U(r)$. In this first paper we therefore ignore the real part of $V(r)$ which is very sensitive to the energy dependence of Γ_G^*. We find that the imaginary part of Eq. (10) is fairly insensitive to Γ_G^*:[23]

$$W(r)=W(0)\rho^2(r),\quad W(0)=-\frac{16}{3}\frac{\alpha_S^*}{\pi}g_G\int_0^\infty dq\,\mathbf{q}^2\frac{M_G^*\Gamma_G^*}{[\mathbf{q}^2-(E_0+\bar{E}_0)^2+M_G^{*2}]^2+M_G^{*2}\Gamma_G^{*2}}\,. \tag{11a}$$

Typical density functions $[W(r)/W(0)]^{1/2}$ are shown in Fig. 4 and are compared to the phenomenological Wood-Saxon form of Bryan and Phillips (Dover and Richard use an identical r dependence). This is our main result.

The annihilation process of two $q\bar{q}$ pairs annihilating into two gluons, Fig. 1(c) has also been calculated and gives a radial dependence $\sim\rho^4(r)$ which drops much faster with increasing r than the curves in Fig. 4. Figure 4 shows that our annihilation "range" is r dependent, unlike, e.g., Refs. 25 and 26. If we use this function alone and try to find one annihilation strength [constant multiplying $\rho^4(r)$] that fits $p\bar{p}$ elastic *and* charge-exchange scattering data at the same energy we do not succeed. The forward slope of elastic $p\bar{p}$ is affected if this strength is too large for the $\rho^4(r)$, but this strength is necessary in order to have at least a forward shoulder in the charge-exchange cross section. With the imaginary potential of (11a) we can reproduce data reasonably well as presented in Sec. III. If we change the short-range r dependence of $\rho^2(r)$ with the restriction that $\rho^2(0)=1$ we find that the calculated $d\sigma/d\Omega$ is not changed even if we deviate strongly from the $\rho^2(r)$ behavior for $r\lesssim 0.5$ fm. [The strength of the imaginary potential compared to the real meson-exchange potential has to be constant in order to reproduce the total cross sections, therefore $\rho(0)=1$.] But $d\sigma/d\Omega$ is changed if we change the $\rho^2(r)$ behavior for $r>0.5$ fm. This indicates that the $N\bar{N}$ scattering is sensitive to the r dependence of $W(r)$ for values of r between 0.5 fm and up to 2 fm beyond which $W(r)$ becomes essentially zero (see Fig. 4 and discussion in Sec. III). This is consistent with the findings of Alberg *et al.*[12] It suggests that the annihilation process of Fig. 1(c) with its "range" given by $\rho^4(r)$ has an effective strength (for $N\bar{N}$ scattering) not much larger than the strength $W(0)$ for the pro-

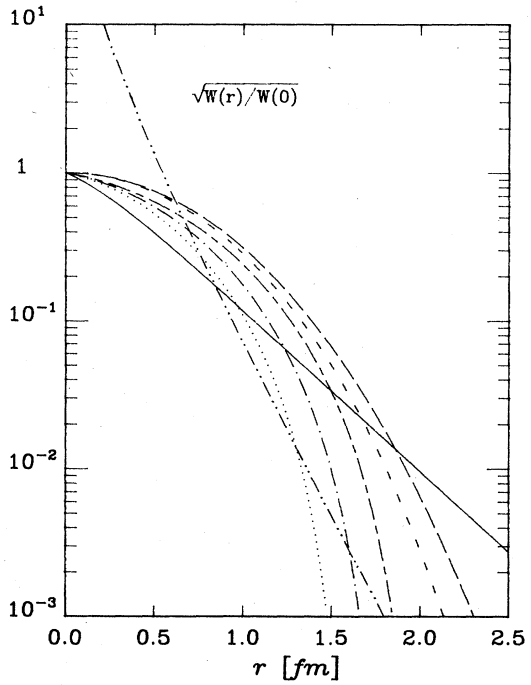

FIG. 4. $[W(r)/W(0)]^{1/2}$ versus r for various quark models: scalar confinement potentials $M(r)=c_n r^n$ (long-dashed curve, $n=2$, $c_2=805$ MeV fm^{-2}; short-dashed curve, $n=3$, $c_3=930$ MeV fm^{-3} [Refs. 19(d) and 19(e)]), and the MIT bag model (short-dashed—long-dashed $R_{\rm bag}=1$ fm; dotted-dashed, $R_{\rm bag}=0.9$ fm; dotted, $R_{\rm bag}=0.8$ fm); also shown is the corresponding Wood-Saxon form (solid line), see text. The corresponding curve for the Paris annihilation potential (Ref. 25) $W(r)\sim K_0(2mr)/r$ is plotted as the dashed—double-dotted curve, and is much steeper than the Wood-Saxon slope.

cesses of Figs. 1(a) and 1(b), which have a longer "range" determined by $\rho^2(r)$ (see Fig. 4). This study has demonstrated that the effective r-dependent annihilation "range" around 0.7 to 1.5 fm cannot be much shorter than what is displayed in Fig. 4. The annihilation process where all three $q\bar{q}$ pairs annihilate into three gluons (a disconnected quark line diagram) is $\sim\rho^6(r)$ and has an even shorter "range." We find that this $\rho^6(r)$ behavior alone cannot describe the $d\sigma/d\Omega$'s either. This must therefore also be strongly suppressed relative to the $\rho^2(r)$ processes. In other words, we show in our phenomenological analysis that this last annihilation process, which is a disconnected diagram in the topological quark picture, is suppressed. In the limit $\Gamma_G^*\to 0$ we obtain from Eq. (11a) the very simple result which we will use to estimate a value for $W(0)$,

$$W(0)=-\tfrac{8}{3}\alpha_s^* g_G[(E_0+\bar{E}_0)^2-M_G^{*2}]^{1/2}\ . \qquad (11b)$$

Here the quark and antiquark energies E_0 and $\bar{E}_0$ are simply their energy eigenvalues $E_{1/2}$ which they attain as a result of their confinement in the rest system of N and $\bar{N}$, i.e., $E_0=\bar{E}_0=E_{1/2}\approx 500$–$600$ MeV after c.m. corrections.[19(b)] In the $N\bar{N}$ center-of-mass system the quark and antiquark will have an additional energy which depends on the $N\bar{N}$ c.m. momentum such that the energy will be given roughly by $E_0=\bar{E}_0=[E_{1/2}+\frac{1}{9}\mathbf{p}_{\text{c.m.}}^2]^{1/2}$. With this relation we obtain for Eq. (11b)

$$W(0)=-\tfrac{8}{3}\alpha_s^* g_G[4E_{1/2}^2+\tfrac{4}{9}\mathbf{P}_{\text{c.m.}}{}^2-M_G^{*2}]^{1/2}\ . \qquad (12)$$

Our annihilation strength is energy dependent. A rough estimate of this strength gives at $|\mathbf{P}_{\text{c.m.}}|=326$ MeV/c ($P_{\text{lab}}=690$ MeV/c) $W(0)=-2.5$ GeV ($M_G^*=1$ GeV, $g_G=5,\alpha_s^*=0.4$) whereas for the parameters $M_G^*=0$, $g_G=1,\alpha_s^*=0.4$, as an extreme case, we obtain $W(0)=-1.3$ GeV. In the following we will use this annihilation model with $W(0)$ as a free parameter together with three different OBEP's to describe $p\bar{p}$ scattering data.

III. CALCULATIONAL RESULTS

We have used the one-boson-exchange potentials (OBEP's) of Bryan and Phillips,[15] of Nijmegen model[16] D, and of Richard[17] together with the optical potential, Eq. (11), derived from quark-gluon dynamics to describe $p\bar{p}$ scattering data. We have used $W(0)$ of Eq. (11) as a free parameter.

Our results are shown in Figs. 5–9. In Figs. 5 and 6 we show for two quark potential models, with r^3 or r^2 dependence how the differential cross sections for antiproton momentum $p_{\text{lab}}=690$ MeV/c change with the free parameter $W(0)$ when we use the Bryan-Phillips velocity-dependent OBEP. In Figs. 5(a) and 6(a) for elastic $p\bar{p}$ scattering we see a strong dependence on $W(0)$ for scattering angles $\theta_{\text{c.m.}}\gtrsim 90°$ whereas the charge exchange shows only a slight dependence on $W(0)$. It should here be remarked that with a value of $W(0)=-1$ GeV we can describe the elastic scattering very well for both the r^2 and r^3 quark potential models whereas the charge exchange will only have a shoulder instead of the dip-bump structure in Figs. 5(b) and 6(b) for *both* potential shapes.

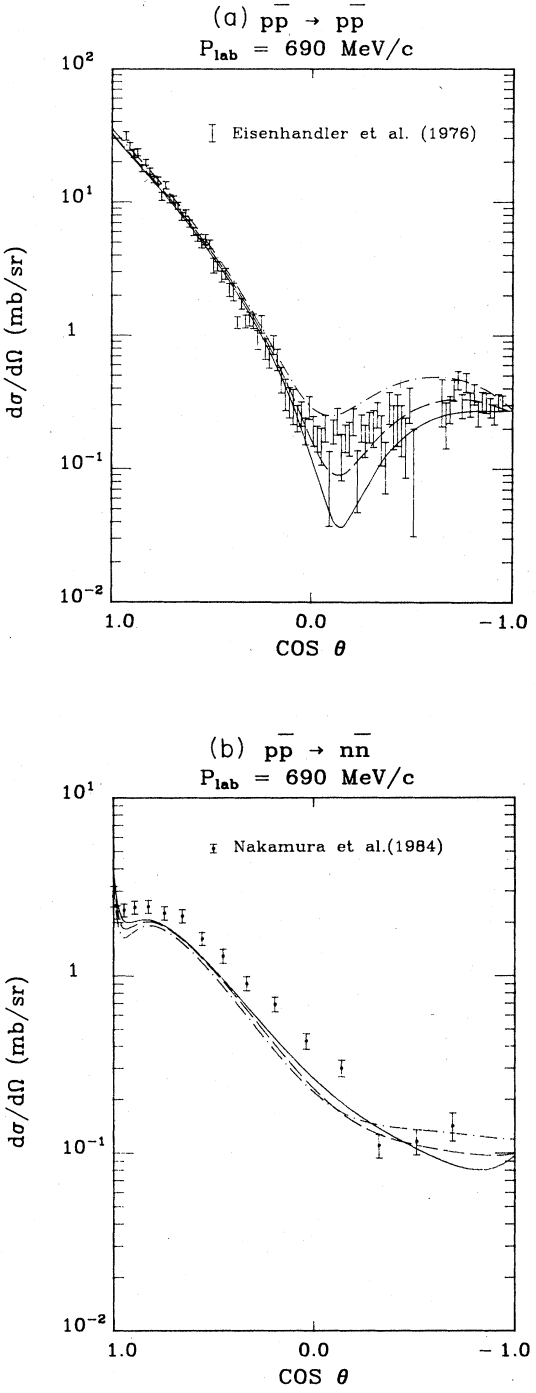

FIG. 5. (a) $p\bar{p}$ elastic scattering at $p_{\text{lab}}=690$ MeV/c, data are from Ref. 27. The Bryan-Phillips OBEP is combined with the quark potential $M(r)=c_3r^3$, $c_3=930$ MeV fm^{-3}, for different annihilation strength, see text: solid curve, $W(0)=-2.5$ GeV; dashed curve, $W(0)=-4.1$ GeV; dashed-dotted curve, $W(0)=-7.5$ GeV. (b) $p\bar{p}\to n\bar{n}$ at $p_{\text{lab}}=690$ MeV/c, data are from Ref. 28. We have renormalized these data to the total charge-exchange cross section of Hamilton *et al.* (Ref. 29). The curves are as in (a).

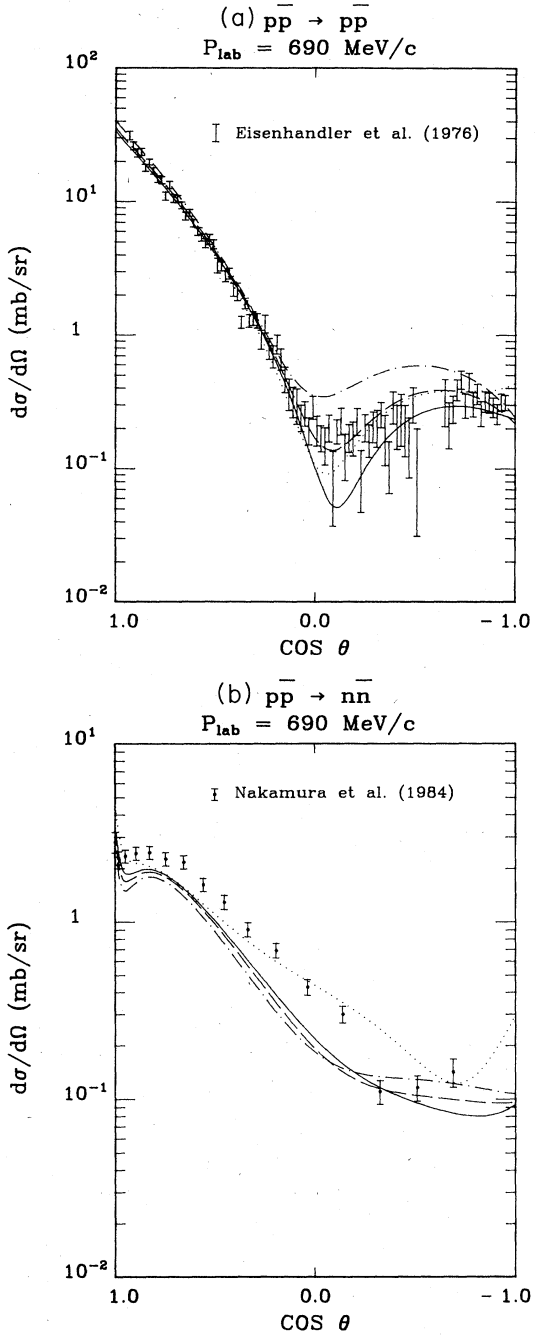

FIG. 6. (a) Curves and data as in Fig. 5(a) but with the quark potential $M(r)=c_2r^2, c_2=805$ MeV fm^{-2}. The dotted curve is for $W(0)=-1.0$ GeV. (b) $p\bar{p}\rightarrow n\bar{n}$ curves as in (a) and data as in Fig. 5(b). The dotted curve is for $W(0)=-1.0$ GeV.

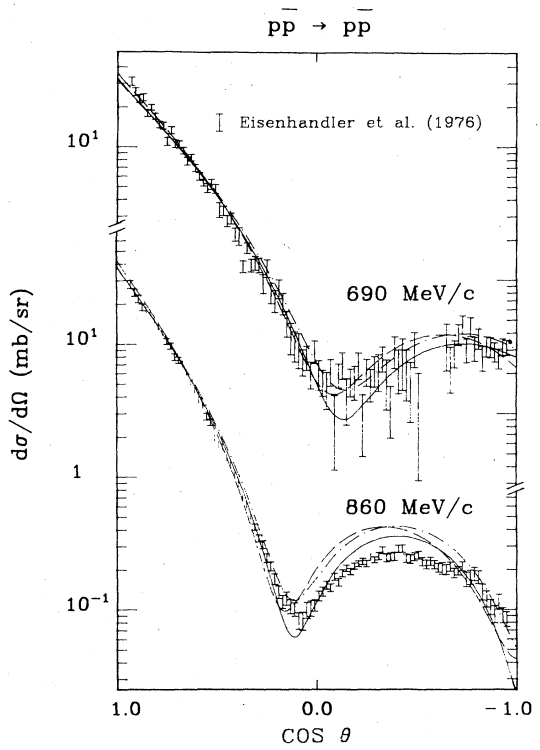

FIG. 7. $p\bar{p}$ elastic at $p_{lab}=690$, 860 MeV/c with "best fits" from Figs. 5(a) and 6(a) compared with the MIT-bag-model ($R_{bag}=1$ fm) result; solid curve, $M=c_3r^3, W(0)=-4.1$ GeV; dashed curve, $M=c_2r^2, W(0)=-4.1$ GeV; dashed-dotted curve, MIT bag $W(0)=-7.5$ GeV; data are taken from Ref. 27.

In Fig. 7 we have plotted the elastic $d\sigma/d\Omega$ again using the Bryan-Phillips OBEP with the "best fitted" value of $W(0)$ for the different quark model wave functions including the MIT quark wave function with a bag radius of 1 fm. A smaller bag size (0.8 or 0.9 fm) produces only a shoulder in the charge exchange and much less backward structure in elastic scattering, unless one is willing to admit a much larger annihilation strength $W(0)$ which will damp out the heavier boson exchanges compared to the pion-exchange. As seen in Fig. 4 we here explore mainly how quickly the annihilation potentials decrease for large $N\bar{N}$ distances. Keep in mind that all three quark models give the same nucleon-charge rms radius. In Figs.(8a) and 8(b) we compare our three quark models with the new charge-exchange data of Nakamura *et al.*[28] at five energies. It is clear that the quark wave-function models from the two potentials are very similar (both give a quark core contribution to the proton rms radius of 0.65 fm before recoil and c.m. corrections), but none of the three curves describes the detailed structure of the data very well. And finally in Figs. 9(a) and 9(b) we compare elastic and charge exchange $d\sigma/d\Omega$ with our quark potential wave functions of two values of $W(0)$ and two different meson-exchange models, the static Paris $N\bar{N}$ model of Richard and the OBEP Nijmegen model D. The elastic $d\sigma/d\Omega$ can be well described for a value of $W(0)$ depending on the meson-exchange model used whereas both meson exchange models have a too pronounced forward dip-bump structure for the charge-exchange reaction compared to the data of Nakamura *et al.*[28] This dip-bump structure is not very pronounced in the Bryan-Phillips

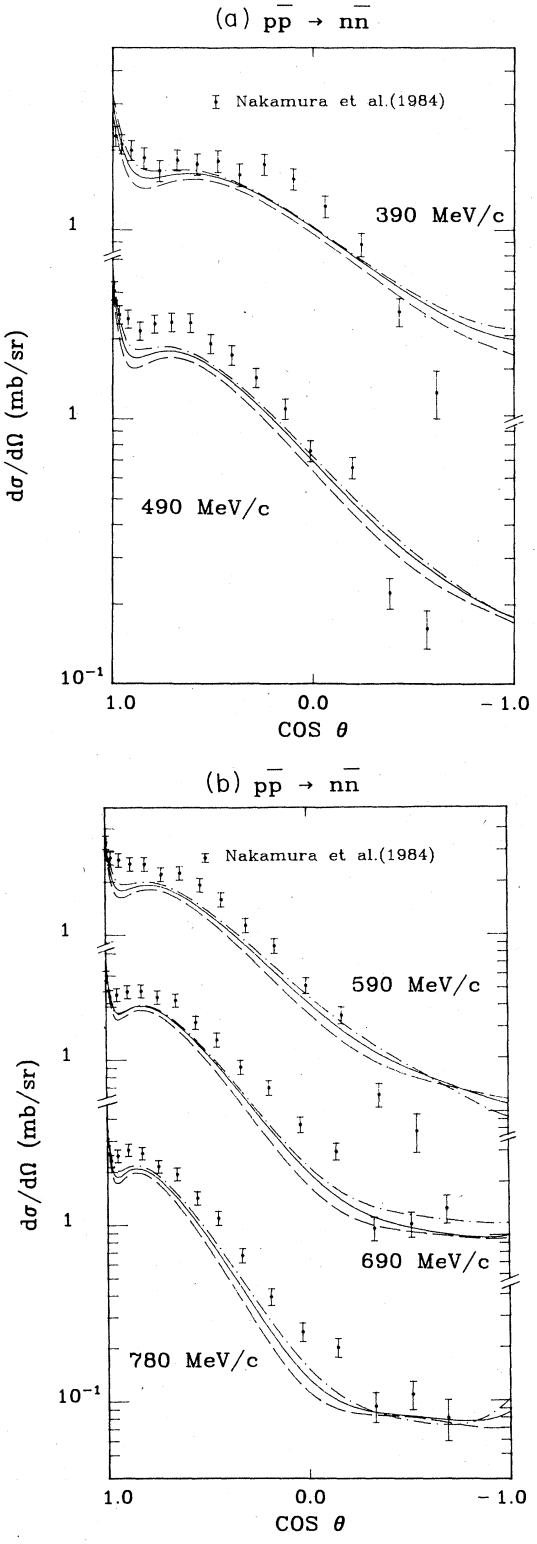

FIG. 8. $p\bar{p} \rightarrow n\bar{n}$, at $p_{lab} = 390, 490, 590, 690, 780$ MeV/c. Data are from Ref. 28. We have renormalized these data to the total charge-exchange cross section of Hamilton *et al.* (Ref. 29). The curves are as in Fig. 7.

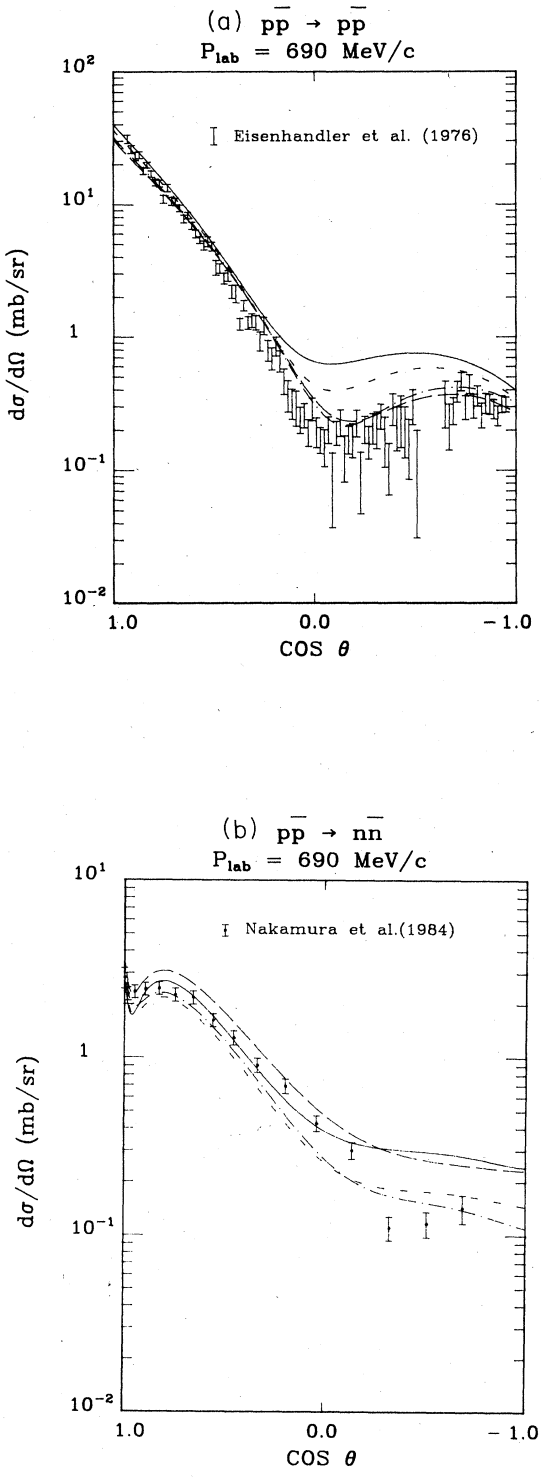

FIG. 9. (a) $p\bar{p}$ elastic at $p_{lab} = 690$ MeV/c, data are from Ref. 27. The quark potential $M(r) = c_3 r^3, c_3 = 930$ MeV fm^{-3}, is combined with two OBEP's, each with two different $W(0)$; see text. Dover-Richard OBEP: $W(0) = -10$ GeV (solid), -2.5 GeV (long-dashed). Nijmegen model-D OBEP: $W(0) = -7.5$ GeV (short-dashed), -4.1 GeV (dashed-dotted). (b) $p\bar{p} \rightarrow n\bar{n}$ at $p_{lab} = 690$ MeV/c, data as in Fig. 5(b) and curves as in (a).

OBEP as seen in Fig. 8, but as discussed in Ref. 9 the forward charge-exchange reaction is sensitive to the differences in the meson-exchange models.

IV. DISCUSSION AND CONCLUSIONS

We have here presented a calculation of antiproton-proton scattering with an annihilation potential given by predetermined quark wave functions. These quark wave functions, which follow from the long-range QCD forces, reproduce in chiral models the nucleon charge radius and give the "range" of the $p\bar{p}$ annihilation potential. As seen from Fig. 4 this "range" is r dependent. The strength of this potential is given by the hard, short-range processes of one $q\bar{q}$ pair annihilating into one or more gluons, which processes all have the same radial dependence in the coherent approximation. We have here kept the strength $W(0)$ of this potential as a free parameter. In our calculation we also find that the disconnected "quark-line" annihilation diagrams are suppressed as discussed in Sec. II. To test this annihilation model and the approximations employed in calculating the curves in Fig. 4, we have to calculate the meson annihilation channels using the same approximations that lead to Eq. (10) and Fig. 4. This should also enable us to be more specific regarding the real part of the annihilation potential.

ACKNOWLEDGMENTS

We are grateful to Dr. K. Nakamura for communicating to us the KEK data prior to publication and to Dr. J. M. Richard for providing us with his $N\bar{N}$ potential.[17] Helpful discussions with Dr. C.B. Dover, Dr. S. Kahana, Dr. R. Vinh Mau, and Dr. J. M. Richard are gratefully acknowledged. This research has been partially supported by Deutsche Forschungsgemeinschaft Grant No. Te 102/2-2 (R.T.), the U.S. DOE Grant No. DE-FG05-84 ER 40143 (T.M.), and NSF Grant No. Phys. 82-01910 (F.M.).

[1]C. G. Callan, R. F. Dashen, and D. J. Gross, Phys. Lett. **78B**, 307 (1978); Phys. Rev. D **19**, 1826 (1979).

[2]G. E. Brown and M. Rho, Phys. Lett. **82B**, 177 (1979); A. Chodos and C. B. Thorn, Phys. Rev. D **12**, 2733 (1975); T. Inoue and T. Maskawa, Prog. Theor. Phys. **54**, 1833 (1975).

[3]A. W. Thomas, Adv. Nucl. Phys. **13**, 1 (1983).

[4]F. Myhrer, in *International Review of Nuclear Physics,* edited by T. T. S. Kuo (World Scientific, Singapore, 1984), Vol. 1.

[5]W. Weise, in *International Review of Nuclear Physics* (Ref. 4), Vol. 1.

[6]A. Martin, Phys. Rev. **124**, 614 (1961).

[7]Yu. A. Simonov, Phys. Lett. **107B**, 1 (1981); in *Few Body X,* proceedings of the Tenth International IUPAP Conference, Karlsruhe, 1983, edited by B. Zeitnitz [Nucl. Phys. **A416**, 109c (1984)], Vol. 1, p. 109; E. L. Lomon, in *Few Body X,* Vol. 2, p. 609.

[8]O. D. Dalkarov and F. Myhrer, Nuovo Cimento **40A**, 152 (1977); F. Myhrer, in *Nucleon-Nuclon Interactions—1977,* proceedings of the Second International Conference, Vancouver, edited by H. Fearing, D. Measday, and A. Strathdee (AIP, New York, 1973), p. 357, and references therein.

[9]T. Mizutani, F. Myhrer, and R. Tegen, Phys. Rev. D **32** 1663 (1985).

[10]M. Maruyama and T. Ueda, Nucl. Phys. **A364**, 297 (1981); Phys. Lett. **124B**, 121 (1983); Osaka University Report No. OUAM 84-6-2, 1983 (unpublished).

[11]A. M. Green, J. A. Niskanen, and J. M. Richard, Phys. Lett. **121B**, 101 (1983); A. M. Green and J. A. Niskanen, Nucl. Phys. **A412**, 448 (1984); in *International Review of Nuclear Physics* (Ref. 4), Vol. 1; A. M. Green, J. A. Niskanen, and S. Wycech, Phys. Lett. **139B**, 15 (1984).

[12]R. A. Freedman *et al.*, Phys. Rev. D **23**, 1103 (1981); M. Alberg *et al.*, *ibid.* **27**, 536 (1983).

[13]A. Faessler, G. Lübeck, and K. Shimizu, Phys. Rev. D **26**, 3280 (1982).

[14](a) G. C. Rossi and G. Veneziano, Nucl. Phys. **B123**, 507 (1977); (b) E. Witten, *ibid.* **B160**, 57 (1979); (c) G. C. Rossi, in *Physics at LEAR with Low Energy Cooled Antiprotons,* proceedings of the Workshop, Erice, 1982, edited by U. Gastaldi and R. Klapisch (Plenum, New York, 1984); (d) C. B. Dover and P. M. Fishbane, Nucl. Phys. **B244**, 349 (1984).

[15]R. A. Bryan and R. J. N. Phillips, Nucl. Phys. **B5**, 201 (1968); R. A. Bryan and B. L. Scott, Phys. Rev. **177**, 1435 (1969).

[16]M. M. Nagels, T. A. Rijken, and J. J. de Swart, Phys. Rev. D **12**, 744 (1975).

[17]J. M. Richard (private communication); see also C. B. Dover and J. M. Richard, Phys. Rev. C **21**, 1466 (1980).

[18]T. A. DeGrand *et al.*, Phys. Rev. D **12**, 2060 (1975).

[19](a) W. Weise and E. Werner, Phys. Lett. **101B**, 223 (1981); (b) R. Tegen, R. Brockmann, and W. Weise, Z. Phys. A **307**, 339 (1982); (c) R. Tegen, M. Schedl, and W. Weise, Phys. Lett. **125B**, 9 (1983); (d) R. Tegen and W. Weise, Z. Phys. A **314**, 357 (1983); (e) E. Oset, R. Tegen, and W. Weise, Nucl. Phys. **A426**, 456 (1984).

[20]W. Marciano and H. Pagels, Phys. Rep. **36C**, 137 (1978).

[21]R. L. Jaffe and K. Johnson, Phys. Lett. **60B**, 201 (1976); J. F. Donoghue *et al.*, Phys. Lett. **99B**, 416 (1981); H. Høgaasen and J. Wroldsen, Phys. Lett. **116B**, 369 (1982); C. E. Carlson *et al.*, Phys. Rev. D **27**, 1556 (1983); **28**, 2895(E) (1983); J. F. Donoghue, *ibid.* **29**, 2559 (1984).

[22]F. Lenz and E. Moniz, Adv. Nucl. Phys. **13** (1983); E. Oset, H. Toki, and W. Weise, Phys. Rep. **83**, 281 (1982).

[23]We have numerically tested that the r dependence coming from the gluon propagator alone is very slow compared to the r dependence from $\rho^2(r)$. For $M_G^*=1$ GeV and $\Gamma_G=0.1$ or 0.01 GeV we found a very weak r dependence ($\sim 15\%$ variation between 0 fm and 1 fm).

[24]F. Myhrer and R. Tegen, Phys. Lett. B (to be published).

[25]J. Coté *et al.*, Phys. Rev. Lett. **48**, 1319 (1982); B. Loiseau, in *Proceedings of the Third LAMPF II Workshop, Los Alamos, 1983,* edited by John C. Allred (Los Alamos National Laboratory, Los Alamos, 1983).

[26]P. H. Timmers *et al.*, Phys. Rev. D **29**, 1928 (1984).

[27]E. Eisenhandler *et al.*, Nucl. Phys. **B113**, 1 (1976).

[28]K. Nakamura *et al.*, Phys. Rev. Lett. **53**, 885 (1984).

[29]R. P. Hamilton *et al.*, Phys. Rev. Lett. **44**, 1179 (1980).